http://dx.doi.org/10.14500/aro.12493

Flexural Strengthening of Self-Compacting Reinforced Concrete L-Shaped Columns with Carbon Fiber: Experimental Study

Ziyad A. Hamad† and Sinan A. Yaseen

Department of Civil Engineering, College of Engineering, Salahaddin University - Erbil, Kurdistan Region – F.R. Iraq

***Abstract*—Reinforced concrete (RC) columns are fundamental structural elements in buildings responsible for transferring loads from superstructures to the foundations. Improving their performance under different load conditions is important for ensuring structural safety and long-term durability, particularly to increase the flexural strength of columns. Because carbon fiber-reinforced polymer (CFRP) composites are so strong, lightweight, corrosion-resistant, and simple to install, they should be used instead of traditional strengthening methods. This study examines the flexural strengthening of self-compacting RC L-shaped columns under axially and biaxially eccentric loads by using longitudinally applied CFRP. Six cases of columns in total were prepared and tested, including three unstrengthened columns and three flexurally strengthened with CFRP, which were tested at eccentricities ($e_x = e_y$) of 0 mm (pure axial load), 50 mm, and 100 mm. The experimental findings showed that various loading conditions led to different failure processes. While concentrically loaded specimens failed suddenly as a result of brittle concrete crushing and reinforcement bar buckling, columns subjected to eccentric loading showed combined flexural-compression failure characterized by tension-side cracking, lateral displacement, and compression-side concrete crushing. There is less impact on increasing axial capacity at ($e_x = e_y = 0$), with an improvement of roughly 6%. The load capacity improved by up to 27% at ($e_x = e_y = 50$ mm) and 39% at ($e_x = e_y = 100$ mm) under eccentric loading. These results show that loading situations have a major impact on the performance of CFRP, with flexural improving moment capacity, ductility, and fracture control under eccentric loads.**

***Index Terms*—L-shaped column, Biaxial-eccentric loading, Carbon fiber-reinforced polymer strengthening, Flexural performance, Self-compacting concrete.**

I. Introduction

Columns are critical structural components that transmit building loads to the foundation. In specific layouts, irregular shapes such as L- or T-sections are used, especially at corners or near elevator shafts, where standard column forms are impractical. L-shaped reinforced concrete (RC) columns present complex analysis and design challenges due to their irregular geometry and asymmetric stress distribution under axial and eccentric loading (Ramamurthy and Khan, 1983). The sectional characteristics of special-shaped columns such as L columns, are different in comparison to those of conventional rectangular and circular columns, with their influence on load and moment carrying capacities mainly because the center of gravity for L columns lies outside the section (Nayak and Shetty, 2018). The equivalent square method is a simplified method to overcome the difficulty of analyzing irregular column sections, which has been a constant concern for a structural engineer, to design a safe and economical structure in modern buildings and bridge piers. This method works only if they have equal leg dimensions. For unequal leg dimensions, the results are not safe (Al-Ansari, Afzal and Afzal, 2019). Self-compacting concrete (SCC) is a material having outstanding properties that flows and fills formwork without vibration, improving workability, durability, and efficiency (Meko, Ighalo, and Ofuyatan, 2021). It was developed by Professor Hajime Okamura in Japan in the late 1980s (Okamura and Ouchi, 2003). The performance of existing RC columns has been improved by retrofitting techniques, especially in older or seismically subjected structures. Due to its high strength and low weight, carbon fiber-reinforced polymer (CFRP) wrapping improves ductility, load capacity, and resilience to seismic and environmental effects. Additional CFRP layers enhance performance, and CFRP straps perform better than horizontal wraps in high eccentricity situations, even when eccentricity weakens the column (Widiarsa and Hadi, 2013). This study evaluates CFRP flexural strengthening on self-compacting RC (SCRC) L-shaped columns under axial and biaxial eccentric loads, focusing on the interaction between CFRP and loading, failure modes, and improvements in capacity and ductility. The strength increased in FRP-confined rectangular and square columns, while CFRP confinement minimizes the effect of increasing aspect ratio in RC columns, which typically lowers the peak stress (Moussa, et al., 2025). The partial confinement using horizontal strips provides

ARO-The Scientific Journal of Koya University
Vol. XIV, No.1 (2026), Article ID: ARO.12493, 10 pages
DOI: 10.14500/aro.12493
Received: 01 August 2025; Accepted: 11 April 2026
Regular research paper; Published: 12 June 2026
†Corresponding author's e-mail: ziyad.hamad@su.edu.krd

clear gains (≈50%) and enhanced deformation, proving to be an effective substitute for full confinement. Full CFRP confinement significantly increases the strength and ductility of concrete columns, with compressive strength increasing by up to 89% (Dahmani, et al., 2025). Fiber properties and application methods affect the efficiency of CFRP in column reinforcement, and external FRP systems and SCC can improve structural performance (Sikora and Ostrowski, 2025). RC columns with CFRP strips placed between steel hoops demonstrated improved compressive performance and deformation capacity because of their uniform confinement. Thinner CFRP layers and closer strip spacing significantly increased strength and ductility, and an updated model was proposed to precisely estimate the final axial strain (Wang, et al., 2024). The efficiency of different wrapping mechanisms under concentric loading was confirmed by experimental results, which showed that CFRP confinement greatly increased the load-carrying capacity of short, low-strength concrete columns, with strength increases ranging from 35% to 90% (Al-Khafaji, 2023). Near-surface-mounted carbon fiber strips combined with external wrapping greatly improved the strength and ductility of RC columns under axial and uniaxial bending loads (Abokwiek, et al., 2021). Both uniaxial and biaxial loading were applied to CFRP-wrapped RC rectangular columns to evaluate partial and full confinement as well as the precision of design specifications. Axial stiffness, load capacity, and reinforcing strain all increased, while initial stiffness improved by 17% for partial confinement and 37% for full confinement for both forms of confinement. Reinforcement yielding was postponed by CFRP, and load capacity rose by 31% and 33%, respectively. As confinement and eccentricity rose, so did the vertical CFRP strain. Full confinement had safety factors ranging from 1.87 to 2.09, although partial confinement had lower safety factors under biaxial stress (1.55–1.76) than under uniaxial loading (1.93–1.98), indicating the need for more research (Tin, Thuy, and Seo, 2021). Eccentric loading was applied to three rectangular RC columns, two of which were partially covered in CFRP and one of which was unstrengthened. Tensile yielding and concrete crushing caused all columns to fail through compression-controlled modes. While flexural stiffness was only marginally impacted, partial CFRP wrapping significantly increased curvature capacity and post-peak ductility. Furthermore, decreasing stiffness decline following peak load, it enhanced structural durability (Nguyen, Pham, and Tran, 2021). Axial and biaxial bending tests were conducted on four rectangular RC columns reinforced with CFRP. While transverse fibers had minimal impact, longitudinal fibers increased strength and ductility. After yielding till CFRP rupture, the reinforced columns showed an improved load capacity. Tension regulated the development of cracks along the weak axis. CFRP improved stiffness, energy dissipation, and compressive and flexural capability (Rahai and Akbarpour, 2013). The effects of load eccentricity, CFRP layers, and vertical straps were investigated in sixteen square RC columns reinforced with CFRP. Vertical straps increased ductility at high eccentricity, while several CFRP layers increased strength and ductility, especially under eccentric loads. With the exception of pure axial stress, their strength prediction model closely matched experimental findings (Hadi and Widiarsa, 2012). Combining longitudinal and circumferential CFRP wrapping is advised for eccentrically loaded columns. CFRP strengthening improves column performance, especially with moderate eccentricity. At higher eccentricities, its effect is reduced because tensile failure becomes more common (Waryosh, Rasheed, and Al-Musawi, 2012).

II. Materials and Methods

The test specimens consisted of 6 L-shaped concrete columns measuring 1400 mm in total height and 200 × 200 × 100 mm in cross-section, and the column section (excluding brackets) is 900 mm in length. Because the specimens' slenderness ratio (kl/r) was 16.28, or <22 according to ACI 318–19, the column could be designated as a short column (ACI-318, 2019). To provide biaxial-eccentric loading, the heads of each column have been strengthened and extended at both ends. As shown in Fig. 1, each specimen is built with enlarged end brackets that measure 250 mm in length and 250 mm in cross-section to avoid the ends failing earlier than necessary.

Table I displays the two groups into which the tested specimens were divided. Three similarly RC columns with various degrees of biaxial eccentricity, 0, 50, and 100 mm (where ex = ey), were included in each group.

The kind of polymer that is reinforced with carbon fiber (CFRP) strengthening and the quantity of applied biaxial eccentricity are listed in the specimen labels. For example, specimen FL-E100 represents a column confined with CFRP in the flexural direction and subjected to a biaxial eccentric

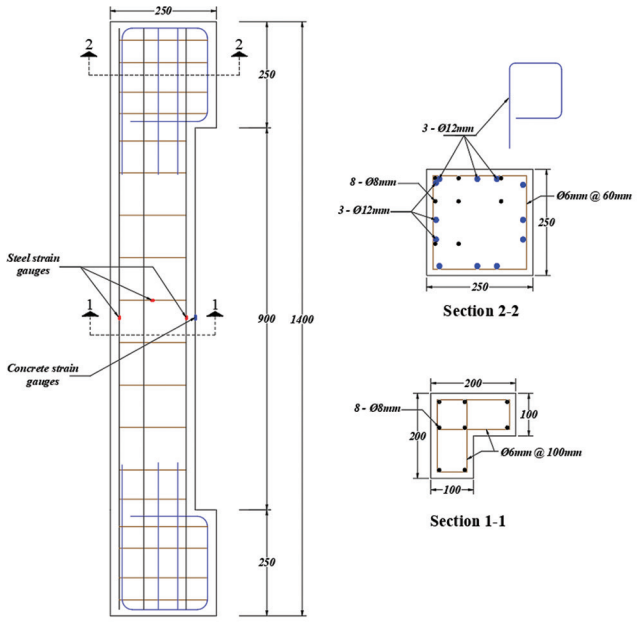

Fig. 1. Details of the column steel reinforcement specimens (as defined in mm).

 http://dx.doi.org/10.14500/aro.12493

TABLE I
Details of Proposed Specimens

No.	Group	Specimen	ρ %	Longitudinal reinforcement	Tie reinforcement	e_x=e_y (mm)	CFRP applied
1	1	C-E0	1.34	8Ø8 mm	Ø6@100 mm	0	…
2		C-E50	1.34	8Ø8 mm	Ø6@100 mm	50	…
3		C-E100	1.34	8Ø8 mm	Ø6@100 mm	100	…
4	2	FL-E0	1.34	8Ø8 mm	Ø6@100 mm	0	Flexural
5		FL-E50	1.34	8Ø8 mm	Ø6@100 mm	50	Flexural
6		FL-E100	1.34	8Ø8 mm	Ø6@100 mm	100	Flexural

CFRP: Carbon fiber-reinforced polymer

load of 100 mm in both directions (e_x = e_y), but specimen C-E0 represents a control column without CFRP confinement under concentric loading.

Three concrete columns without CFRP strengthening became part of the first group (control specimens), which was reinforced with 8–Ø8 mm longitudinal steel bars and Ø6 mm steel ties placed 100 mm apart. The column end brackets are reinforced additionally with 3–Ø12 mm longitudinal steel bars in each direction and Ø6 mm ties at 60 mm spacing. Three concrete columns made up the second group, which were strengthened in the flexural direction by one layer of CFRP and supported by the same longitudinal steel bars and ties spaced 100 mm apart.

Fig. 1 shows the size and details of the reinforcement used in the tested specimens. All the experimental works were carried out in the Civil Engineering Department's concrete lab, Salahaddin University-Erbil.

Based on the 100 mm × 200 mm cylinder samples, the average concrete compressive strength was 36.6 MPa (ASTM-C39, 2021). According to (ASTM-A615, 2020), the tie and longitudinal reinforcements were 6 mm and 8 mm deformed steel bars with 587 and 515 MPa for ultimate strengths and 551 and 355 MPa for yield strengths.

The final mix proportions of the components used for producing SCC are shown in Table II. The standard ordinary Portland cement (Type I), manufactured in Tasluja, Al-Sulaymaniyah, Iraq, was used. Sika ViscoCrete-171 Precast, a third-generation polycarboxylate-based superplasticizer, was used as a high-range water-reducing addition to make SCC more workable and flowable.

Table III presents the acceptance criteria for SCC. These ratios have been determined while the fresh characteristics described in Table IV were evaluated using the standard SCC tests (EFNARC, 2002; ACI-237R-07, 2007); the fresh properties tests are shown in Fig. 2.

All of the concrete columns' formwork was created from plywood sheets. The steel ties and reinforcements were put together and fastened in the shape. All specimens had 15 mm clear covers applied to the ties' faces.

As shown in Fig. 3, a standard steel reinforcement cage was put together for the specimens. On level ground, the formwork molds were positioned horizontally. Without a vibrator, after pouring concrete into the formwork. In order to maintain moisture conditions, the control specimens and columns were covered with nylon and moist burlap after being cast at the same time. According to (ASTM-C31/C31M, 2019), the curing process continued for 28 days.

TABLE II
Mix Proportion Control of the Concrete Mixture by the Weight

Mixing proportions of self-concrete kg/m^3						
Cement	Limestone Powder	Sand	Gravel	Water	W/C	Superplasticizer
340	60	950	880	156	0.55	1%

TABLE III
Criteria for Self-Compacting Concrete Acceptance (Efnarc, 2002)

No.	Method	Unit	Typical range of values	
			Minimum	Maximum
1	Slump flow by the Abrams cone	mm	650	800
2	T50	sec	2	5
3	J-Ring	mm	0	10
4	L-Box	(H_2/H_1)	0.8	1
5	V-Funnel	sec	6	12
6	Time increase, V-funnel at $T_{5\,min}$	sec	0	+3

TABLE IV
Fresh Properties of Scc

Slump flow (mm)	T50 (sec)	J-Ring (mm)	L-Box (H_2/H_1)	V-Funnel (s)	V-Funnel T5 min (s)
650	2.8	9.6	0.88	6.7	1.86

SCC: Self-compacting concrete

Before applying the CFRP fiber, the column spacemen's surface was cleaned, and the edges were chamfered. Apply just one layer of CFRP in the flexural direction as shown in Fig. 4.

In this study, unidirectional Profiber CW300, manufactured by DCP Company, was utilized to reinforce the column using Quickmast ER350 resin. The fiber's thickness was 0.166 mm, and its stiffness and tensile strength were 4800 MPa.

To prevent bearing failure at the ends, the enlarged ends of each column have been protected by a 100 mm-high CFRP. To provide even force distribution from the machine to the column surface, capping was placed on each column specimen's bottom and top ends with rubber that is 8 mm thick (Othman and Mohammad, 2019).

The column specimens were approached with a pin connected at both ends. To make sure that the column was vertically aligned, extra attention was required. A 50 mm diameter steel ball with three 10 mm holed plates which were welded to a 40 mm plate's top and bottom to give it eccentricity as shown in Fig. 5. To measure longitudinal bar strain using two strain gauges for the long sides of tie reinforcement, the electric resistance strain gauges are

Fig. 2. Self-compacting concrete fresh tests.

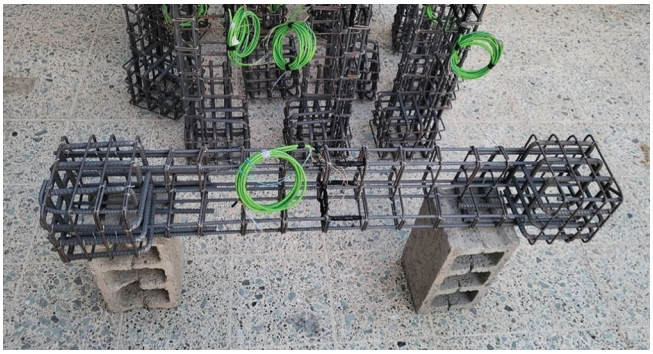

Fig. 3. Spacemen reinforcement cage.

attached to the center of longitudinal bars, one on the tension side and one on the compression side, as shown in Fig. 1.

To measure the concrete compression strain, another strain gauge was fixed to the column's mid-height compression face. To measure the column's lateral displacement in the X and Y directions during the loading stage, two linear variable differential transformers (LVDTs) were also placed at mid-height. During the specimen testing procedure, the LVDT and electrical strain gauges were additionally connected to the data acquisition system (data logger) to record the load value, deflection, longitudinal reinforcement strain, and concrete strain, respectively.

III. Results and Discussion

The test results for CFRP-flexurally strengthened and unstrengthened RC L-shaped columns are presented in this section. All of the columns were loaded to failure to determine their maximum load-carrying capacity. Throughout the procedure, the testing apparatus continuously recorded the necessary information. The main findings, including the maximum load, are listed in Table V. The structural behavior, failure modes, longitudinal reinforcement strain, lateral deflection, and the influence of various factors on the columns' maximum load capacity are all covered in the discussion that follows.

A. Failure Modes and Behavior

The column specimens that were subjected to concentric loading generally failed suddenly and without any obvious cracks, deflection, or warning. However, concrete crushing on the compression face, followed by obvious lateral displacement and cracking on the face of tension, created eccentric loading on the columns (50 mm and 100 mm) to fail. In general, for both groups at higher eccentricity

TABLE V
Experimental Test Results

No.	Group	Specimen	ρ %	CFRP applied (one layer)	$e_x=e_y$ (mm)	P_{max} (kN)
1	1	C-E0	1.34	…	0	1178
2		C-E50	1.34	…	50	390
3		C-E100	1.34	…	100	122
4	2	FL-E0	1.34	Flexural	0	1256
5		FL-E50	1.34	Flexural	50	496
6		FL-E100	1.34	Flexural	100	170

CFRP: Carbon fiber-reinforced polymer

($e_x = e_y = 100$ mm), these failure indicators were noticeably more noticeable than at lower eccentricity ($e_x = e_y = 50$ mm).

Concentric loading columns ($e_x = e_y = 0$)

Concentric loading columns ($e_x = e_y = 0$). No visible cracks appeared in specimens C-E0 and FL-E0 as the load increased to their failure point. At failure, the concrete abruptly and explosively crushed near the mid-height, resulting in sudden and unexpected failure. This crushing was followed by the longitudinal reinforcement bars buckling, as shown in Fig. 6. Specimen C-E0 failed at mid-height with concrete crushing at a load of 1178 kN, while FL-E0 exhibited a similar failure mode at a slightly higher load of 1256 kN. These results suggest that flexural strengthening had a minimal impact on the columns' capacity to support loads and did not change the overall failure mode.

Columns with medium eccentric loading ($e_x = e_y = 50$ mm)

Columns subjected to eccentricity ($e_x = e_y = 50$ mm) displayed markedly different behavior and strength compared to those under concentric loading. In specimen C-E50, the first horizontal crack on the tension side appeared at a load of 210 kN, followed by progressive crack widening and concrete crushing at mid-height, leading to failure at 390 kN. In contrast, specimen FL-E50, strengthened with CFRP, showed delayed crack visibility and failed at a higher load of 496 kN due to combined concrete crushing and CFRP rupture. These results confirm the effectiveness of flexural strengthening in enhancing load-carrying capacity under eccentric loading. As shown in Fig. 7, the mode of failure and crack pattern of column specimens. Because specimen FL-E50 was a CFRP-wrapped flexural portion, the external confinement prevented the first crack and its spread from being visually observed. At a higher load, the specimen failed due to CFRP rupture and parallel concrete crushing on the compression face. Under the CFRP, tension cracks were discovered by post-failure inspection. While cracks were more extensively distributed

http://dx.doi.org/10.14500/aro.12493

Fig. 4. Applying carbon fiber-reinforced polymer to flexural direction of columns.

Fig. 5. Set up of the column specimen, the loading plates and steel balls that can be set in x and y directions using a self-leveling digital laser to provide a certain eccentricity with respect to the longitudinal axis of the column are indicated by the blue frames.

throughout the tension face in the control specimen, the crack pattern was concentrated in the mid-height region.

Columns with high eccentric loading ($e_x = e_y = 100$ mm)

Columns tested under higher eccentric loading ($e_x = e_y = 100$ mm) exhibited significantly different behavior

Fig. 6. Mode of failure of column specimens ($e_x = e_y = 0$).

and strength compared to those under concentric loading and lower eccentricity ($e_x = e_y = 50$ mm). At a load of 77 kN, the first horizontal crack in specimen C-E100 developed on the tension face. As the load increased, the cracks gradually widened and extended, while in FL-E100, CFRP wrapping delayed crack visibility. With increased loading, cracks extended along the tension face and became more pronounced. Failure occurred due to concrete crushing, above mid-height in C-E100 and below mid-height in FL-E100. C-E100 failed at 122 kN, while FL-E100 failed at 170 kN, including CFRP rupture. As shown in Fig. 8, the mode of failure and crack pattern of column specimens. Because of the exterior confinement, the first crack and its spread were invisible for specimen FL-E100, which had been entirely wrapped in CFRP. Tension cracks were seen beneath the CFRP to failure. The cracks were on the tension face, much like in the control specimen; however, they were primarily localized in the mid-height area rather than being evenly spaced.

B. Load-Strain Behavior of Column Specimens

Each specimen of the six tested columns had four strain gauges attached to it, with three extra gauges provided as standbys. Every one of the four main strain gauges worked as intended and recorded data during the loading procedure. A steel strain gauge (St2) was fixed to a longitudinal bar at the tensioned corner, a concrete compressive strain gauge (St1) was placed on the compression face, a steel strain gauge (St3) was fixed to a longitudinal bar at the compression corner, and a tie reinforcement strain gauge (St4) was attached to the tie along the longer side. Tensile deformation is indicated by positive strain values, and compressive deformation is indicated by negative strain values.

Fig. 7. Mode of failure and crack pattern of column specimens ($e_x = e_y = 50$ mm).

Fig. 8. Mode of failure and crack pattern of column specimens ($e_x = e_y = 100$ mm).

Pure axial loading ($e_x = e_y = 0$) was applied to columns C-E0 and FL-E0. The load-strain curves in Fig. 9 show that St1 was under compression and is linear at low load. However, when specimens reach near their maximum capacity, the curves flatten out, indicating yielding or significant internal cracking before failure. The concrete compressive strain (St1) of both specimens remained below the maximum value of 0.003 specified by the (ACI-318, 2019) code. In the end, both column specimens failed due to a sudden crushing. Columns C-E50 and FL-E50 were tested under biaxial eccentric loading with ($e_x = e_y = 50$ mm). St1 was compressed. As specified by (ACI-318, 2019), the concrete compressive strain (St1) in specimen C-E50 reached a maximum value of 0.003 at failure. However, specimen FL-E50 displayed larger strains beyond 0.003 under biaxial loading, which can be related to the flexural CFRP confinement, which raised the strain capacity of the columns. Columns C-E100 and FL-E100 displayed a flexure-dominated response when subjected to biaxial eccentric loading with ($e_x = e_y = 100$ mm). The load-strain curves in Fig. 9 show St1 compression. Every specimen's concrete compressive strain (St1) remained below the code's ultimate limit of 0.003 (ACI-318, 2019), showing that longitudinal steel stress rather than concrete crushing was the reason for failure. Flexural confinement (FL-E100) increased the failure loads to 170 kN, while the control specimen C-E100 failed at 122 kN. These results indicate that flexural confinement improves flexural capacity more effectively.

The load–longitudinal steel tension strain relationship in Fig. 10 illustrates the tensile response of the reinforcement under loading. Pure axial loading (ex = ey = 0) was applied to columns C-E0 and FL-E0. St2 in compression is represented by the load-strain curves, as shown in Fig. 10. Although the overall concrete strain did not reach 0.003, the control column (C-E0) and specimen FL-E0 displayed higher steel strains above 0.002 under pure axial loading. Localized deformations and small eccentricities that led to unbalanced stress distribution and strain concentration in

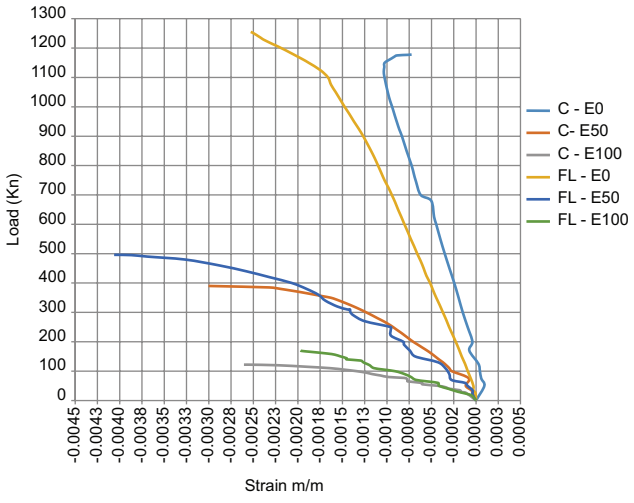

Fig. 9. Load – concrete compressive strain (St1) curve for column specimens under various loading.

http://dx.doi.org/10.14500/aro.12493

the reinforcement could have been the cause of this. In the end, both columns failed due to a sudden crushing. Columns C-E50 and FL-E50 were tested under biaxial eccentric loading with ($e_x = e_y = 50$ mm). Tension was detected by St2. Specimen FL-E50 displayed greater steel stresses beyond 0.003 during biaxial loading, which can be related to the flexural CFRP strengthening that raised the strain capacity of the columns. St2 failed (FL-E50 at 496 kN and C-E50 at 390 kN). In the control specimen C-E50, St2 yielded at 200 kN, showing a usual tension-controlled response. With flexural confinement (FL-E50), the yielding loads improved to 270 kN, demonstrating improved flexural performance. Columns C-E100 and FL-E100 displayed a flexure-dominated response when subjected to biaxial eccentric loading with ($e_x = e_y = 100$ mm). Tensile strain was applied to St2 based on the load-strain curves as shown in Fig. 10. Every specimen's concrete compressive strain (St1) remained below the code's ultimate limit of 0.003 (ACI-318, 2019), indicating that longitudinal steel stress instead of concrete crushing was the cause of failure. In the control specimen C-E100, St2 failed at 122 kN after yielding at 55 kN. Performance differences can be seen when comparing the CFRP strengthening configurations: Flexural strengthening (FL-E100) enhanced the failure loads to 170 kN. These findings demonstrate that at high eccentricity, flexural strengthening is more effective in increasing flexural capacity and delaying steel yielding.

The compressive strain response (St3), illustrated in Fig. 11, indicates the ductility and crushing behavior of the specimens under investigation. Pure axial loading ($e_x = e_y = 0$) was applied to columns C-E0 and FL-E0. Fig. 11's load-strain curves show that St3 was under compression. Under pure axial load, specimen FL-E0 displayed higher steel strains above 0.002, but the control column (C-E0) showed lower steel compressive strain. Specific deformations and small eccentricities that led to uneven stress distribution and strain concentration in the reinforcement could have been the cause of this. In the end, a sudden crushing caused both columns to fail. Columns C-E50 and FL-E50 were subjected to biaxial eccentric loading with ($e_x = e_y = 50$ mm). St3 was compressed. The flexural CFRP strengthening, which raised the columns' strain capacity, explains why specimen FL-E50 displayed higher steel strain above 0.003 at failure. St3 failed (FL-E50 at 496 kN and C-E50 at 390 kN). In the control specimen C-E50, St3 gave at 260 kN, indicating a typical tension-controlled response. With flexural confinement (FL-E50), the yielding loads improved to 310 kN, demonstrating improved flexural performance. Columns C-E100 and FL-E100 showed a flexure-dominated response when subjected to biaxial eccentric loading with ($e_x = e_y = 100$ mm). The load-strain curves in Fig. 8 showed that St3 was compressed. In the control specimen C-E100, the St3 failed at 122 kN after yielding at 110 kN. Performance changes can be seen when comparing the CFRP confinement configurations: Flexural confinement (FL-E100) increased the failure loads to 170 kN. These results demonstrate that under high eccentricity, flexural confinement is more effective in increasing flexural capacity and delaying steel yielding.

The strain response (St4) of the steel ties is shown in Fig. 12, which shows that every column specimen had the St4 in tension under various loading conditions. Pure axial

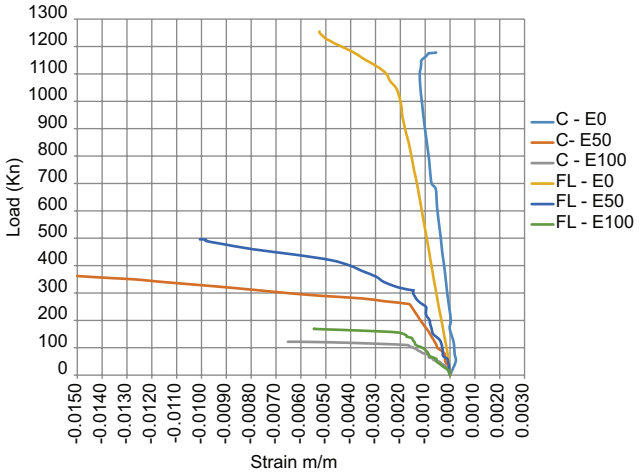

Fig. 11. Load – longitudinal steel compressive strain (St3) curve for column specimens under various loading.

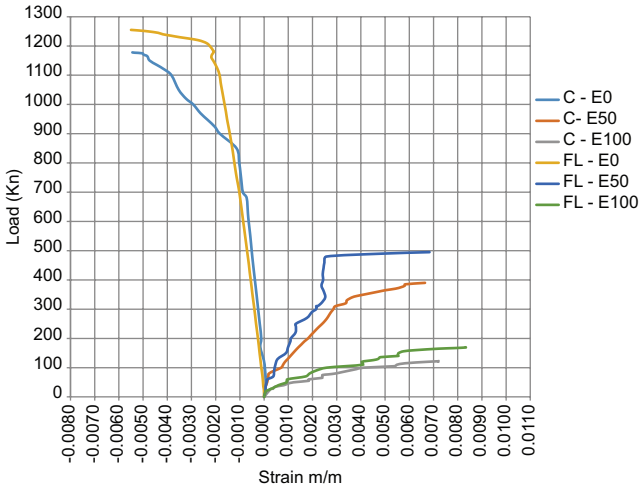

Fig. 10. Load – longitudinal steel tension strain (St2) curve for column specimens under various loading.

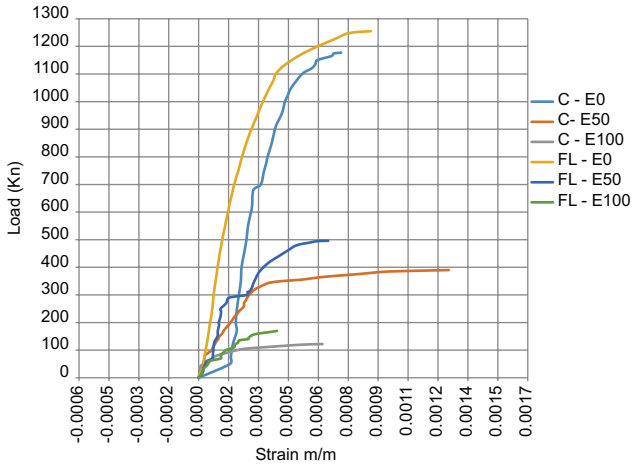

Fig. 12. Load –steel tie strain (St4) curve for column specimens under various loading.

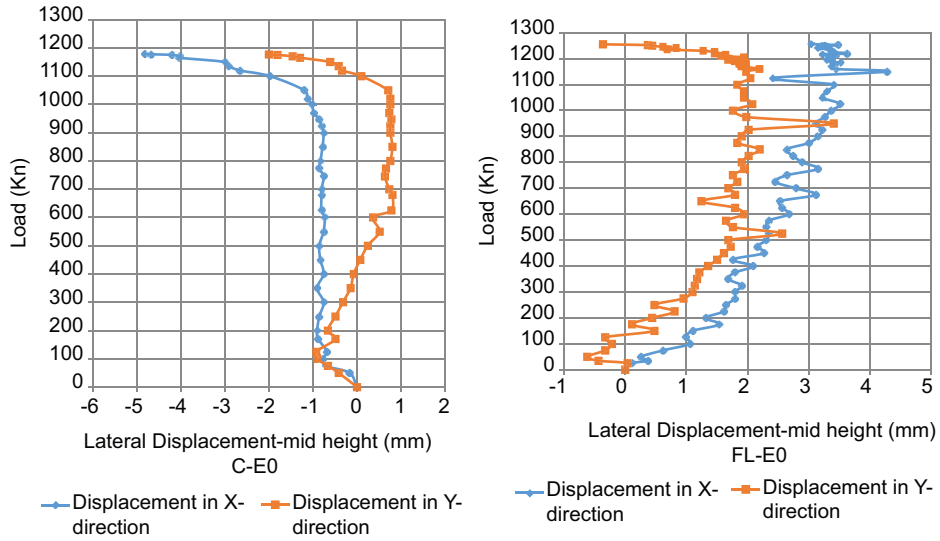

Fig. 13. Load – Lateral displacement curve for column specimens (C-E0 and FL-E0).

loading ($e_x = e_y = 0$) was applied to columns C-E0 and FL-E0. St4 on the ties was tension, as seen by the load-strain curves in Fig. 12. During the pre-peak load period, the strains in the tie reinforcement reached and exceeded their maximum values, but they stayed linear. Columns C-E50 and FL-E50 were subjected to biaxial eccentric loading with ($e_x = e_y = 50$ mm). Up until the peak load, St4 on the ties displayed minimal strain. A small tensile strain of roughly 0.001 was found at failure, indicating a minor contribution to the ties under the current eccentricity. Columns C-E100 and FL-E100 displayed a flexure-dominated response when subjected to biaxial eccentric loading with ($e_x = e_y = 100$ mm). The load-strain curves in Fig. 12 show that the transverse reinforcement contributed very little to the applied eccentricity, with just a little tensile strain of roughly 0.00068 found at failure and stresses in the transverse ties, St4, being negligible until close to peak load.

C. Lateral Displacement

The load-lateral displacement responses of the tested columns were analyzed to investigate the effects of eccentric loading and CFRP strengthening on the structural stiffness and deformation capacity. The load-displacement curves show that the CFRP-strengthened specimens perform very differently from the control specimens under various loading conditions.

For concentrically loaded specimens C-E0 and FL-E0, lateral displacements were minimal, indicating mostly axial compression and no bending. The load-lateral displacement curves for all control (C) and CFRP flexural-strengthened (FL) specimens subjected to axial load ($e_x = e_y = 0$) are shown in Fig. 13. The load-displacement curves showed an almost vertical rise to the ultimate load, followed by an abrupt failure caused by crushed concrete and buckling reinforcement. CFRP has little effect on lateral displacement under concentric pressure because of its mostly flexural contribution. However, FL-E0 attained a slightly greater ultimate load (1256 kN) than C-E0 (1178 kN), indicating a minor increase in axial capacity and insignificant constriction of the concrete core without significantly altering the brittle failure behavior.

The load-lateral displacement curves for all control (C) and CFRP FL specimens subjected to an eccentricity of ($e_x = e_y = 50$ mm) are shown in Fig. 14. The load-displacement behavior was significantly changed when using a 50 mm biaxial eccentricity. The combined axial and bending effects were reflected in the rising lateral displacements that both C-E50 and FL-E50 displayed with load. With a strong post-peak decline from compression zone crushing and increased displacement from tensile cracking, C-E50 showed a nonlinear reaction. The CFRP-strengthened FL-E50, on the other hand, showed improved ductility and structural performance with smaller lateral displacements, a greater ultimate load (496 kN vs. 390 kN), a larger peak displacement, and a more progressive post-peak decrease.

At the maximum eccentricity of 100 mm, flexural impacts predominated, with CFRP strengthening having the largest impact. The load-lateral displacement curves for all control (C) and CFRP flexural-strengthened (FL) specimens subjected to an eccentricity of ($e_x = e_y = 100$ mm) are shown in Fig. 15. The control specimen C-E100 obtained an average ultimate load of 122 kN with progressively increasing lateral displacements, progressive cracking, and compression zone crushing. By achieving a higher ultimate load of 170 kN, a larger peak displacement, and improved post-peak behavior, the CFRP-strengthened FL-E100, on the other hand, showed superior ductility. Its load-displacement curve remained above C-E100, indicating effective tensile stress resistance, controlled crack propagation, and sustained residual capacity.

At the end, eccentricity increased lateral displacement and decreased load capacity. Higher load resistance and delayed stiffness decrease were demonstrated by CFRP-strengthened columns; the strengthening effect was particularly noticeable at eccentricities of 50 and 100 mm.

http://dx.doi.org/10.14500/aro.12493

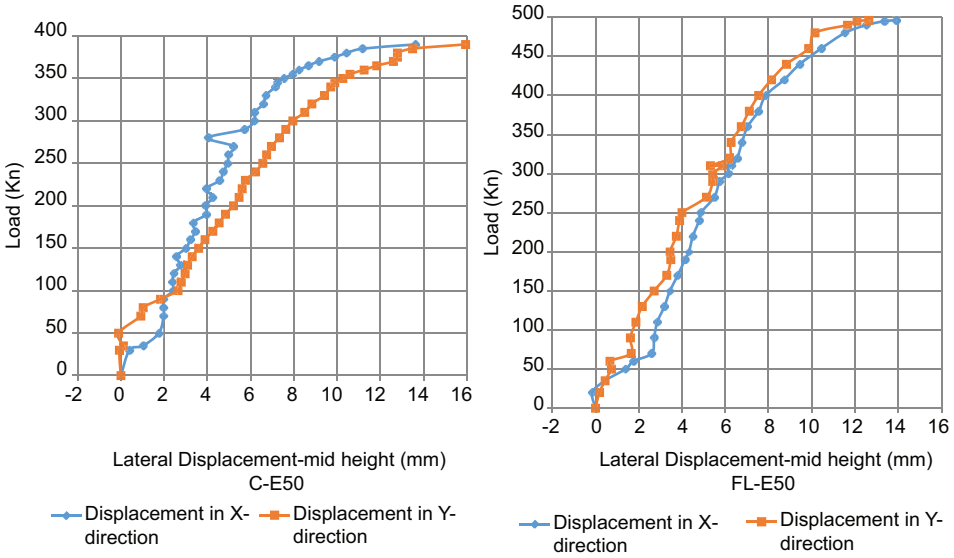

Fig. 14. Load – Lateral displacement curve for column specimens (C-E50 and FL-E50).

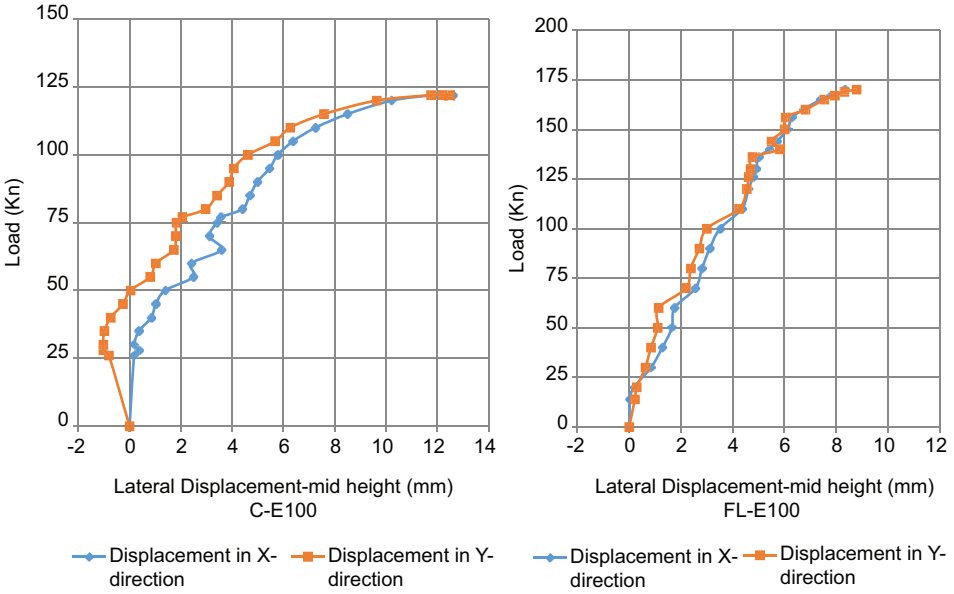

Fig. 15. Load – Lateral displacement curve for column specimens (C-E100 and FL-E100).

IV. Conclusion

In this experimental investigation, the structural performance of L-shaped columns of SCRC reinforced with CFRP applied longitudinally was tested under each axial and biaxial-eccentric loading condition. The following are the investigation's main conclusions:

1. The load-carrying capacity of L-shaped columns was greatly improved by flexural CFRP strengthening, especially when eccentric loading was applied. At eccentricities of 50 mm and 100 mm, respectively, the strengthened columns showed load increases of approximately 27% and 39% compared to the unstrengthened specimens.
2. Failure modes were clearly influenced by loading conditions and strengthening configuration. CFRP strengthened delayed crack propagation, controlled lateral deformation, and led to more stable failure patterns.
3. Strain measurements indicated increased ductility in CFRP-strengthened columns. While the tie bar strain was higher in strengthened columns, it showed minimal variation with changes in eccentricity, suggesting a limited impact of eccentricity on the effectiveness of transverse reinforcement.
4. Analysis of lateral displacement verified CFRP's contribution to increased stiffness. Even at high eccentricity, strengthened columns exhibited improved flexural stiffness and lateral stability with less movement and more symmetry in both the X and Y directions.

Overall, the results indicate that applying CFRP longitudinally is an effective retrofit method for enhancing the flexural strength, ductility, and stability of L-shaped RC columns, especially when subjected to complex biaxial-eccentric loading. The behavior of irregular column

geometries is better understood due to this work, which additionally supports the wider use of CFRP materials for strengthening structural components in existing structures, particularly those that are subject to eccentric loads.

References

Abokwiek, R., Abdalla, J.A., Hawileh, R.A., and El MAaddawy, T., 2021. RC columns strengthened with NSM-CFRP strips and CFRP wraps under axial and uniaxial bending: Experimental investigation and capacity models. *Journal of Composites for Construction*, 25, p.04021009.

ACI-237R-07., 2007. *Self-Consolidating Concrete (ACI 237R-07)*. American Concrete Institute, Farmington Hills, MI.

ACI-318., 2019. *Building Code Requirements for Structural Concrete (ACI 318-19) and Commentary*. American Concrete Institute, Farmington Hills, MI.

Al-Ansari, M., Afzal, M., and Afzal, M., 2019. Simplified irregular column analysis by equivalent square method. *Journal of Structural Engineering and Applied Mechanics*, 2, pp.36-46.

Al-Khafaji, Z., 2023. Study the behavior of square reinforced concrete columns strengthened with CFRP. *Electronic Journal of Structural Engineering*, 23, pp.79-84.

ASTM-A615., 2020. *Standard Specification for Deformed and Plain Carbon-Steel Bars for Concrete Reinforcement*. ASTM International, Pennsylvania.

ASTM-C31/C31M., 2019. *Standard Practice for Making and Curing Concrete Test Specimens in the Field*. ASTM International, Pennsylvania.

ASTM-C39., 2021. *Standard Test Method for Compressive Strength of Cylindrical Concrete Specimens*. ASTM International, Pennsylvania.

Dahmani, S., Khitas, N.E.H., Babba, R., Hebbache, K., Douadi, A., Boutlikht, M., Messai, A., and Belebchouche, C., 2025. Carbon fiber-reinforced polymer (CFRP) confinement strategies for concrete columns: Evaluating the efficacy of full and partial wrapping methods. *Metallurgical and Materials Engineering*, 31, pp.238-246.

EFNARC., 2002. *Specification and Guidelines for Self-Compacting Concrete*. Efnarc, Farnham, UK.

Hadi, M.N., and Widiarsa, I.B.R., 2012. Axial and flexural performance of square RC columns wrapped with CFRP under eccentric loading. *Journal of Composites for Construction*, 16, pp.640-649.

Meko, B., Ighalo, J.O., and Ofuyatan, O.M., 2021. Enhancement of self-compactability of fresh self-compacting concrete: A review. *Cleaner Materials*, 1, p.100019.

Moussa, A.M., Abdellatif, M.R., Abdallah, M.S.E., and Farghal, O.A., 2025. Experimental study on the effect of aspect ratio on CFRP-confinement efficiency in rectangular RC columns. *Structural Concrete*, 2025, pp.1-20.

Nayak, V., and Shetty, T., 2018. Analysis of L shaped RC columns subjected to bending with axial load using moment-curvature relationship. *International Journal of Mechanical and Production Engineering Research and Development*, 8, pp.195-206.

Nguyen, T.H., Pham, X.D., and Tran, K.D., 2021. Experimental study on the behavior of eccentrically compressed reinforced concrete columns strengthened with CFRP composite sheets. *Journal of Science and Technology in Civil Engineering (JSTCE)-HUCE*, 15, pp.172-181.

Okamura, H., and Ouchi, M., 2003. Self-compacting concrete. *Journal of Advanced Concrete Technology*, 1, pp.5-15.

Othman, Z.S., and Mohammad, A.H., 2019. Behaviour of eccentric concrete columns reinforced with carbon fibre-reinforced polymer bars. *Advances in Civil Engineering*, 2019, p.1769212.

Rahai, A., and Akbarpour, H., 2013. Biaxially loaded CFRP-confined rectangular RC columns. *Journal of Civil Engineering*, 2, pp.27-31.

Ramamurthy, L., and Khan, T.H., 1983. L-shaped column design for biaxial eccentricity. *Journal of Structural Engineering*, 109, pp.1903-1917.

Sikora, O., and Ostrowski, K.A., 2025. A review of external confinement methods for enhancing the strength of concrete columns. *Materials*, 18, p.3222.

Tin, H.X., Thuy, N.T., and Seo, S.Y., 2021. Structural behavior of RC column confined by FRP sheet under uniaxial and biaxial load. *Polymers*, 14, p.75.

Wang, J., Lu, L., Lu, S., and Yang, J., 2024. Behavior and modeling of partially CFRP confined reinforced concrete columns under axial compression. *Engineering Structures*, 303, p.117466.

Waryosh, W.A., Rasheed, M.M., and Al-Musawi, A.H., 2012. Experimental study of reinforced concrete columns strengthened with CFRP under eccentric loading. *Journal of Engineering and Sustainable Development*, 16, pp.421-440.

Widiarsa, I.B.R., and Hadi, M.N., 2013. Performance of CFRP wrapped square reinforced concrete columns subjected to eccentric loading. *Procedia Engineering*, 54, pp.365-376.